30-mW 690-nm High-Power Strained-Quantum-Well AlGaInP Laser

Yoshiyasu Ueno, Hiroaki Fujii, Hiroyuki Sawano, Kenichi Kobayashi, Kunihiro Hara, Akiko Gomyo, and Kenji Endo

Abstract—**This paper presents a high-power 690-nm AlGaInP laser for use in a high-density rewritable-optical-disk memory system. The deterioration of its temperature characteristics, which results from the high-power-oriented laser structure, is improved by using compressively strained GaInP quantum wells as the active layer. Output power of 40 mW is achieved up to 80°C. Stable fundamental-transverse-mode operation is obtained up to 50 mW. Output-power-induced facet degradation is suppressed by an Al_2O_3 facet coating. The lasers operate stably at 30 mW at 50°C for over 2600 h. The mean extrapolated lifetime is 10 000 h.**

I. Introduction

HIGH-POWER red-light-emitting AlGaInP lasers are attractive light sources for many applications, such as optical-disk memories, and laser printers [1]–[6]. One advantage of AlGaInP lasers is the more than 30% reduction in focused-spot size, due to the shorter laser wavelength, as compared with conventional AlGaAs lasers. This reduced spot size increases the recording density of optical-disk memories by 1.5 times [7], which is very attractive for high-capacity small-size data files, video files, etc.

For practical use, optical-disk-memory systems require a high output power of more than 30 mW up to about 50°C with high beam quality. Compared with AlGaAs lasers, the disadvantage for AlGaInP lasers is the relatively low maximum output power density limited by the catastrophic optical damage (COD) at the mirror facets to 1–2 MW/cm^2 (light density value in vacuum, [2]), which is approximately one third of that obtained for AlGaAs lasers. In attempts to overcome this disadvantage, several kinds of laser structures have been fabricated [1]–[6] and maximum fundamental-transverse-mode output powers up to 60–70 mW have been reported for a window-structure laser [3] and bulk-active-layer lasers [4]. However, long-term 30-mW life-test data at 50°C have only been reported for a few devices [5] and 40-mW life-test data have been reported only up to 40°C [6]. The limitations are the deterioration of temperature characteristics as a result of the high-power-oriented laser structures and output-power-induced gradual degradation at the mirror facets [8], [9].

Manuscript received November 2, 1992; revised February 12, 1993.

The authors are with Opto-Electronics Research Laboratory, NEC Corporation, 34 Miyukigaoka, Tsukuba, Ibaraki 305, Japan.

IEEE Log Number 9209132.

Very recently, the present authors [10] and another group [11] have achieved 30- to 35-mW stable operation at 50°C for high-power AlGaInP lasers with compressively strained QW active layers. The present paper describes the development of the laser in detail and shows its potential for practical use in rewritable-optical-disk memory systems. Threshold current reduction for lasers with the strained QW active layer was previously predicted and reported [12]–[14]. We applied the strained QW active layer to the high-power AlGaInP laser, considering that threshold current reduction should improve the temperature characteristics with reduction in carrier overflow to the cladding layer. We also studied output-power limits for long-term stable operation for high-power AlGaInP lasers, and we found that Al_2O_3 facet coating raises the output-power limit to 60% of the COD limit. The Al_2O_3-coated strained-QW lasers demonstrated 30-mW stable operation at 50°C for over 2600 h.

II. Facet Coating

Output-power dependency of the gradual laser degradation in long-term CW operation was investigated for coated refractive-index-guide AlGaInP lasers with 64-nm-thick bulk-$Ga_{0.5}In_{0.5}P$ active layers. The lasers were mounted to heat sinks on their p-side. Both Al_2O_3-coated lasers and SiO_2-coated lasers were life-tested and then compared. Both kinds of dielectric film were formed in the same magnetron-sputtering apparatus. The measured COD levels of both kinds of coated lasers under CW operation agree with the theoretical levels calculated from the facet reflectivity [15] as listed in Table I. This agreement shows that there was no significant difference between the COD light densities inside the facets of Al_2O_3-coated and SiO_2-coated lasers. The facet reflectivities were derived from the slope efficiencies measured at the coated and uncoated facets of the lasers. These facet reflectivities also agree well with calculations based on the measured thickness and refractive indices of the coating films.

Fig. 1 shows operating current traces for Al_2O_3-coated lasers (Fig. 1(a)) and SiO_2-coated lasers (Fig. 1(b)) under constant-output-power operation at 50°C. SiO_2-coated lasers operated stably at up to 10 mW for over 9000 h. At an output power of 15 mW, which is about two thirds of the COD level, the SiO_2-coated lasers degraded rapidly (all of these lasers suffered from accidental trouble in the

TABLE I
COD LEVELS AND FACET REFLECTIVITIES FOR THE COATED LASERS WITH 64-nm-THICK BULK-GaInP ACTIVE LAYERS AND REFRACTIVE-INDEX-GUIDE STRUCTURES
(The measured COD levels under CW operation of both kinds of coated lasers agree with the theoretical levels calculated from the facet reflectivity.)

Coating Film	Reflectivity (%)	COD Level (mW)
Al_2O_3	5	34
SiO_2	8	20

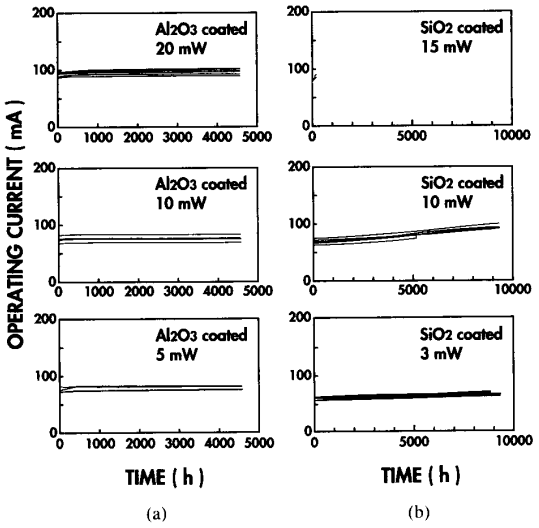

Fig. 1. Operating current traces for coated refractive-index-guide AlGaInP lasers with 64-nm-thick bulk-GaInP active layers under constant-output-power operation at 50°C. The Al_2O_3-coated lasers operated very stably for over 4500 h even at 20 mW. The measured COD levels and facet reflectivities are listed in Table I.

aging aparatus after 173 h of operation). On the other hand, Al_2O_3-coated lasers operated very stably for over 4500 hours even at 20 mW, even though the operating currents were no less than those for the SiO_2-coated lasers operated at 15 mW.

Fig. 2 summarizes the rate of increase in operating current of the SiO_2-coated and Al_2O_3-coated lasers. There was a significant difference in the behavior of the SiO_2-coated laser and the Al_2O_3-coated laser, even though no difference was found in their COD densities, as mentioned above. The SiO_2-coated lasers showed output-power-accelerated degradation. In contrast, the rates of operating-current increase for the Al_2O_3-coated lasers were less than 10^{-5} h^{-1} for output powers up to the output-power-to-COD-limit ratio (P_{OP}/P_{COD}) of 60%. The maximum $P_{OP}/_{COD}$ ratio of 60% is about twice as high as those reported so far [5], [6]. It was speculated that the difference in degradation originates from the greater stability of the interface between an Al_2O_3 film and a semiconductor with a high density of electron–hole pairs excited by the laser light. Thus we chose to use Al_2O_3 coating for our high-power strained QW lasers.

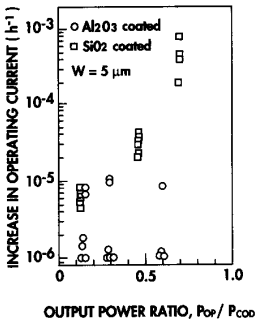

Fig. 2. Rates of increase in operating current for Al_2O_3-coated AlGaInP lasers, life-tested at constant output power (P_{OP}) at 50°C for over 4500 h, compared with those for SiO_2-coated lasers. The Al_2O_3-coated lasers showed very stable operation with operating-current-increase rates of less than 10^{-5} h^{-1} for output powers up to the output-power-to-COD-limit ratio (P_{OP}/P_{COD}) of 60%.

III. STRAINED-QUANTUM-WELL LASER

A. Epitaxial Growth and Fabrication Process

Fig. 3 shows a view of the high-power strained QW AlGaInP laser. The lasers were grown by two-step metalorganic vapor phase epitaxy (MOVPE). In the first step, the following layers were successively grown on a (0 0 1) oriented Si-doped n-GaAs substrate: a Si-doped n-GaAs buffer layer, a 1.5-μm-thick Si-doped n-$(Al_{0.6}Ga_{0.4})_{0.5}In_{0.5}P$ cladding layer ($n \approx 2 \times 10^{17}$ cm^{-3}), an undoped strained QW active layer, a 200-nm-thick Zn-doped p-$(Al_{0.6}Ga_{0.4})_{0.5}In_{0.5}P$ cladding layer ($p \approx 6 \times 10^{17}$ cm^{-3}), a 5-nm-thick Zn-doped p-$Ga_{0.5}In_{0.5}P$ etching-stopper layer, a 1.3-μm-thick Zn-doped p-$(Al_{0.6}Ga_{0.4})_{0.5}In_{0.5}P$ cladding layer ($p \approx 6 \times 10^{17}$ cm^{-3}), a 10-nm-thick Zn-doped p-$Ga_{0.5}In_{0.5}P$ layer, and a 0.25-μm-thick Zn-doped p-GaAs cap layer. The growth conditions were a growth temperature of 660°C, V/III ratios of 150 for GaInP and AlGaInP layers and 50 for GaAs layers, and a growth pressure of 70 torr. Growth rates were 1.8 μm/h for GaInP and AlGaInP layers and 3.0 μm/h for GaAs layers. The source materials were trimethylaluminum, triethylgallium, trimethylindium, dimethylzinc, phosphine, arsine, and disilane [16].

The strained QW active layer consists of 10-nm-thick compressively strained $Ga_xIn_{1-x}P$ wells, separated by 5-nm-thick $(Al_{0.6}Ga_{0.4})_{0.4}In_{0.5}P$ barriers lattice-matched to GaAs. The Ga content (x) for the $Ga_xIn_{1-x}P$ ranged from 0.39 (lattice-mismatch, $\Delta a/a_0 = +1.0\%$) to 0.51 ($\Delta a/a_0 = 0\%$). The number of wells was three or four.

After the first-step growth, a 3- to 4-μm-wide ridge stripe was formed in the [$\bar{1}$ 1 0] direction by chemical etching down to the $Ga_{0.5}In_{0.5}P$ etching-stopper layer. In the second-step growth, a Si-doped n-GaAs current-blocking layer was selectively grown outside the ridge stripe for both fundamental-transverse-mode stabilization and current confinement. The laser cavity length was 700 μm. A 6% Al_2O_3 film was coated on the front facet and a 95% Al_2O_3/amorphous-Si multilayer film was coated on the rear facet.

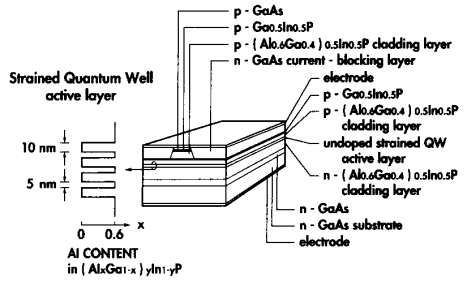

Fig. 3. View of the high-power 690-nm strained QW AlGaInP laser grown by metalorganic vapor phase epitaxy. The strained QW active layer consists of three to four 10-nm-thick $Ga_xIn_{1-x}P$ wells. The Ga content (x) ranged from 0.39 (lattice-mismatch, $\Delta a/a_0 = +1.0\%$) to 0.51 ($\Delta a/a_0 = 0\%$). Fundamental-transverse-mode lasing was stabilized by forming a 3- to 4-μm-stripe waveguide buried by the n-GaAs current-blocking layer. The front facet was coated with a 6% Al_2O_3 film and the rear facet was coated with a 95% Al_2O_3/amorphous-Si multilayer film.

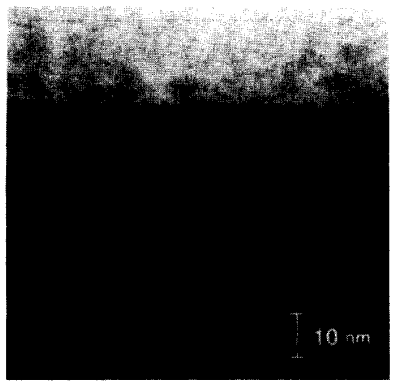

Fig. 4. Dark-field TEM image from [$\bar{1}$ 1 0] direction for the +1.0% lattice-mismatched QW active layer grown on a (0 0 1) oriented GaAs. The interfaces between 10-nm-thick $Ga_{0.39}In_{0.61}P$ wells and 5-nm-thick $(Al_{0.6}Ga_{0.4})_{0.5}In_{0.5}P$ barriers were abrupt, and no dislocation was observed.

B. Strained QW Active Layer

Fig. 4 shows a dark-field transmission electron microscope (TEM) image for the +1.0%-lattice-mismatched QW active layer observed from the [$\bar{1}$10] direction. The dark-contrast regions represent 10-nm-thick $Ga_{0.39}In_{0.61}P$ lattice-mismatched wells, while the light-contrast ones represent 5-nm-thick $(Al_{0.6}Ga_{0.4})_{0.5}In_{0.5}P$ barriers. The interfaces between the strained GaInP wells and the AlGaInP barriers were abrupt. No dislocation was observed.

Fig. 5 shows pulsed threshold current densities (J_{th}) for uncoated 50-μm-wide-stripe strained QW lasers. Pulsed current with a 1-μs pulse width at a 1-kHz repetition was used. The threshold current density decreased with increase in lattice mismatch, and the reduction in threshold current density reached 21% at +1.0% lattice mismatch for 3-well lasers. The bandgap energy also decreased with increase in lattice mismatch at a rate of 98 meV/%, which increased the laser wavelength as shown in Fig. 6.

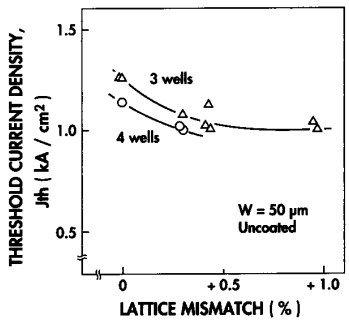

Fig. 5. Pulsed threshold current densities (J_{th}) for the 50-μm-stripe strained QW lasers with three wells (triangles) and four wells (circles). J_{th} decreased with increase in lattice mismatch and the J_{th} reduction reached 21% at +1.0% lattice mismatch for three-well lasers.

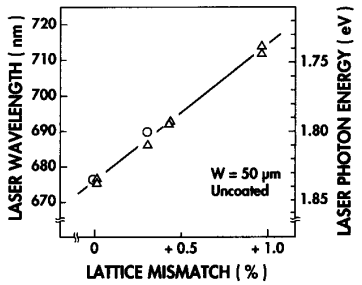

Fig. 6. Laser wavelengths for the strained QW lasers with three wells (triangles) and four wells (circles).

The strained QW active layer improved the temperature characteristics. Fig. 7 shows characteristic temperatures (T_0) for the pulsed threshold current in the 20–50°C range. The characteristic temperature increased with increase in lattice mismatch, and characteristic temperatures for +0.3% to +1.0% lattice-mismatched QW lasers with three wells were 10–33 K higher than those for lattice-matched QW lasers. The improvement in characteristic temperature with increase in lattice mismatch was attributed to both a decrease in injected carrier density in the active layer and an increase in heterobarrier height between the active and cladding layers.

The improvement in characteristic temperature for the strained QW lasers was compared with that for bulk-active-layer lasers. Characteristic temperatures for the strained QW lasers and 20- to 60-nm-thick bulk active-layer lasers are shown in Fig. 8 as a function of threshold nominal current density (J_{th}/d_a). The characteristic temperature noticeably increased with decrese in threshold nominal current density, as was clearly observed for the bulk active-layer lasers. The characteristic temperature increased from 60 K at 160 kA/cm^2 · μm (20-nm-thick active-layer lasers) to 135 K at 22 kA/cm^2 · μm (60-nm-thick active-layer lasers). This indicates the existence of a tradeoff relationship between the characteristic temperature and maximum output power improvements, because expanding the spot size (d/Γ) perpendicular to the junction plane for high-power lasers increases the threshold nominal current density. This tradeoff relationship also applies to the strained QW lasers. However, the relationship was shifted significantly to a higher level with in-

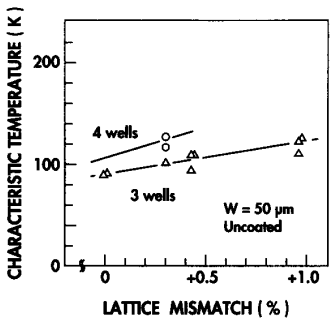

Fig. 7. Characteristic temperatures in the 20–50°C range for the strained QW lasers with three wells (triangles) and four wells (circles). The characteristic temperature increased with increase in lattice mismatch. This improvement was attributed to both a decrease in injected carrier density and an increase in heterobarrier height.

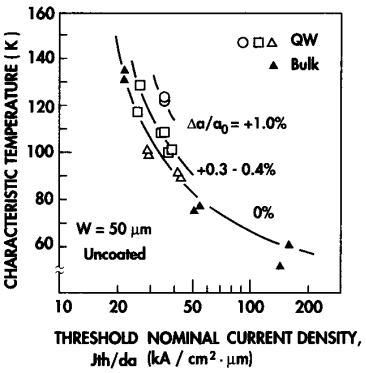

Fig. 8. Characteristic temperatures and threshold nominal current densities for the strained QW lasers (empty triangles: lattice mismatch = 0%; empty squares: +0.3-+0.4%; empty circles: +1.0%), together with those for bulk active-layer lasers (solid triangles: lattice mismatch = 0%) with 20- to 60-nm-thick active layers.

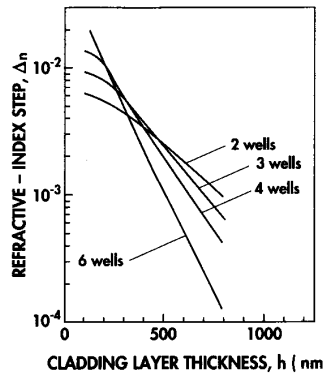

Fig. 9. Calculated refractive-index step for the waveguide of the high-power strained QW lasers as a function of the p-type $(Al_{0.6}Ga_{0.4})_{0.5}In_{0.5}P$ cladding layer thickness outside the stripe (h).

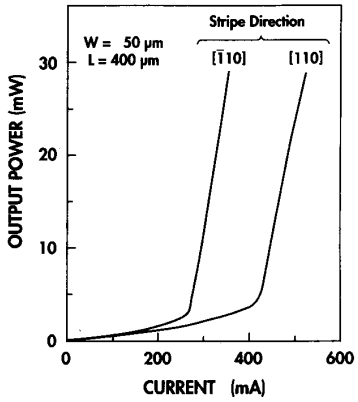

Fig. 10. Output power versus current characteristics for uncoated 50-μm-stripe bulk active-layer lasers [18]. The threshold current for the laser with a [$\bar{1}$ 1 0]-oriented stripe was 0.64 times as low as that for the laser with a [1 1 0]-oriented stripe. This large anisotropy in the threshold current was due to natural superlattice formed in the $Ga_{0.5}In_{0.5}P$ active layer.

crease in lattice mismatch, as seen in Fig. 8. The tendency of characteristic temperature deterioration for high-power lasers is due to an increase in injected carrier overflow to the cladding layer caused by the increase in threshold nominal current density. Thus a reduction in the threshold current density and an increase in the heterobarrier height for the strained QW active layer are favorable for high-power lasers.

C. Waveguide Structure

The waveguide needs a sufficiently large refractive-index step of more than several times 10^{-3} against the carrier-induced refractive-index change [17] to achieve fundamental-transverse-mode stabilization. Fig. 9 shows the calculated refractive-index step for the waveguide of the high-power strained QW lasers. A refractive-index step as large as 10^{-2} was formed by reducing the thickness (h) of the p-type cladding layer outside the stripe to 200 nm. The GaInP etching-stopper layer was used to leave exactly the thin p-type cladding layer outside the stripe after chemical etching. A sufficiently narrow stripe of 3 to 4 μm was applied to prevent higher order transverse-mode lasing.

As we have reported, the stripe direction influences the threshold current density for AlGaInP lasers [18], [19]. Fig. 10 shows output power versus pulsed current characteristics for uncoated 50-μ-stripe bulk active-layer lasers. Threshold curent for the laser with a [$\bar{1}$ 1 0] oriented stripe was 64% that for the laser with a [1 1 0] oriented stripe. This large anisotropy in the threshold current was due to [$\bar{1}$ 1 1] or [1 $\bar{1}$ 1] oriented CuPt-type natural superlattice [20] formed in the $Ga_{0.5}In_{0.5}P$ active layer. Therefore, a [1 1 0] oriented stripe was used to reduce the threshold current density.

IV. Laser Characteristics

Fig. 11 shows CW laser characteristics for the strained QW laser with four +0.30% lattice-mismatched $Ga_{0.47}In_{0.53}P$ wells and a 3- to 4-μm-wide ridge stripe, mounted to a heat sink on its p-side. Fig. 11(a) shows

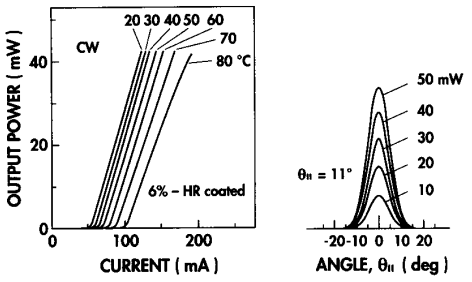

Fig. 11. Continuous-wave laser characteristics for the strained QW laser with four +0.3% lattice-mismatched $Ga_{0.47}In_{0.53}P$ wells. (a) Output power versus current characteristics. The threshold current was 56 mA. The characteristic temperatures were as high as 114 K (20–50°C) and 80 K (50–80°C). (b) Far-field patterns parallel to the junction plane.

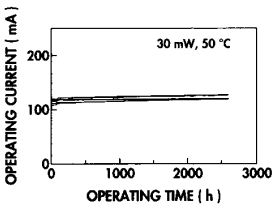

Fig. 12. Operating current traces for the strained QW lasers, life-tested under 30-mW CW constant output power at 50°C. All six lasers operated very stably for over 2600 h. The mean extrapolated lifetime, defined as the operating time at 20% increase in operating current, was 9900 h.

output power versus current characteristics, at temperatures ranging from 25 to 80°C. At 25°C, the threshold current was 56 mA and the slope efficiency was 0.58 W/A. The laser wavelength was 690 nm. The characteristic temperatures were improved to as high as 114 K for 20–50°C and 80 K for 50–80°C. Due to the improvement in characteristic temperature, 40-mW CW output power was achieved up to 80°C. The COD-limited maximum output power was estimated to be 60 mW from the fact that three well lasers have a maximum output power of about 72 mW. The fundamental-transverse mode was obtained up to 50 mW, as shown by the far-field patterns parallel to the junction plane at 10–50 mW in Fig. 11(b). The radiation angles of 11° (parallel to the junction plane) and 24° (perpendicular) resulted in an aspect ratio as low as 2.2.

Fig. 12 shows operating current traces for the strained QW lasers, life-tested under 30-mW CW constant output power at 50°C. A few lasers which showed large degradation during 150-h pre-screening were omitted from this test. As shown in the figure, all six lasers operated very stably for over 2600 h. The operating currents increased at less than $1 \times 10^{-4}\ h^{-1}$, even though the ratio of output power to the COD limit (P_{OP}/P_{COD}) was as high as 50%. The average of the extrapolated lifetimes, defined as the operating time required for a 20% increase in the operating current, was 9900 h. These results demonstrate that these lasers are very promising for use in practical applications.

V. Conclusion

A 30-mW 690-nm strained QW AlGaInP laser with Al_2O_3-coated mirror facets has been successfully developed for use in a high-density rewritable-optical-disk memory system.

The strained QW lasers showed 21% reduction in threshold current density at +1.0% lattice mismatch. Temperature characteristics were improved with increase in lattice mismatch. This improvement was attributed to both a reduction in injected carrier density and an increase in heterobarrier energy. As a result, 40-mW output power was achieved up to 80°C for the strained QW lasers with three +0.3%-lattice-mismatched wells. Stable fundamental-transverse-mode operation was obtained up to 50 mW. The threshold current was 56 mA at 25°C.

In preliminary life tests for bulk active-layer lasers, Al_2O_3-coated lasers showed stable operation for output powers up to an output-power-to-COD-limit ratio of 60%, which is twice as high as previously reported. The Al_2O_3-coated strained QW lasers demonstrated 30-mW stable operation at 50°C for over 2600 h. The mean extrapolated lifetime, defined as the operating time at 20% increase in the operating current, was as long as 10 000 h.

Acknowledgment

The authors wish to thank K. Kobayashi and T. Suzuki for their continuous encouragement. They also acknowledge F. Miyasaka and H. Hotta for their useful comments.

References

[1] H. Fujii, K. Kobayashi, S. Kawata, A. Gomyo, I. Hino, H. Hotta, and T. Suzuki, "High-power operation of a transverse-mode stabilized AlGaInP visible light (λ_L = 683 nm) semiconductor laser," *Electron. Lett*, vol. 23, pp. 938–939, Aug. 1987.

[2] K. Kobayashi, S. Kawata, H. Fujii, I. Hino, A. Gomyo, H. Hotta, and T. Suzuki, "Transverse mode stabilized 670 nm AlGaInP visible-light laser diodes," *Proc. SPIE*, vol. 898, pp. 84–88, Jan. 1988.

[3] Y. Ueno, K. Endo, H. Fujii, K. Kobayashi, K. Hara, and T. Yuasa, "Continuous-wave high-power (75 mW) operation of a transverse-mode stabilized window-structure 680 nm AlGaInP visible laser diode," *Electron. Lett.*, vol. 26, pp. 1726–1727, Sept. 1990.

[4] K. Nitta, K. Itaya, Y. Nishikawa, M. Ishikawa, M. Okajima, and G. Hatakoshi, "High-power (106 mW) CW operation of transverse-mode stabilized InGaAlP laser diodes with strained $In_{0.62}Ga_{0.38}P$ active layer," *Electron. Lett.*, vol. 27, pp. 1660–1661, Aug. 1991.

[5] ——, "Reliable high-power operation of InGaAlP visible light diodes with strained active layer," *Japan. J. Appl. Phys.*, vol. 30, pp. 3862–3864, Dec. 1991.

[6] K. Nitta, M. Okajima, Y. Nishikawa, K. Itaya, and G. Hatakoshi, "Reliable high-power (40 mW) operation of transverse-mode stabilised InGaAlP laser diodes with strained active layer," *Electron. Lett.*, vol. 28, pp. 1069–1070, May 1992.

[7] Y. Yamanaka, K. Kubota, H. Fujii, K. Kobayashi, T. Suzuki, and H. Gokan, "High density magneto-optical recording using 0.67 μm band high power laser diode," *IEEE Trans. Magn.*, vol. 24, pp. 2300–2304, Nov. 1988.

[8] T. Yuasa, M. Ogawa, K. Endo, and H. Yonezu, "Degradation of (AlGa)As DH lasers due to facet oxidation," *Appl. Phys. Lett*, vol. 32, pp. 119–121, Jan. 1978.

[9] K. Itaya, M. Ishikakwa, H. Okuda, Y. Watanabe, K. Nitta, H. Shiozawa, and Y. Uematsu, "Effect of facet coating on the reliability of InGaAlP visible light laser diodes," *Appl. Phys. Lett.*, vol. 53, pp. 1363–1365, Oct. 1988.

[10] Y. Ueno, H. Fujii, H. Sawano, and K. Endo, "Stable 30-mW oper-

ation at 50°C for strained MQW AlGaInP Visible Laser Diodes," *Electron. Lett.*, vol. 28, pp. 860–861, Apr. 1992.
[11] M. Mannoh, S. Kamiyama, J. Hoshina, I. Kidoguchi, H. Ohta, A. Ishibashi, Y. Ban, and K. Ohnaka, "High temperature and high power operation of mode stabilized GaInP/AlGaInP strained MQW lasers," in *Conf. Dig. 13th IEEE Int. Semiconductor Laser Conf.* (Takamatsu, Japan) 1992, paper J4, pp. 186–187.
[12] E. Yablonovitch, and E. O. Kane, "Reduction of lasing threshold current density by the lowering of valence band effective mass," *J. Lightwave Technol.*, vol. LT-4, pp. 504–506, May 1986.
[13] A. R. Adams, "Band-structure engineering for low-threshold high-efficiency semiconductor lasers," *Electron. Lett.*, vol. 22, pp. 249–250, Feb. 1986.
[14] J. Hashimoto, T. Katsuyama, J. Shinkai, I. Yoshida, and H. Hayashi, "Effects of strained-layer structures on the threshold current density of AlGaInP/GaInP visible lasers," *Appl. Phys. Lett.*, vol. 58, pp. 879–880, Mar. 1991.
[15] H. C. Casey and M. B. Panish, *Heterostructure Lasers.* New York: Academic Press, 1978, p. B, ch. 8.
[16] H. Hotta, I. Hino, and T. Suzuki, "Low pressure MOVPE growth of Si-doped $Ga_{0.5}In_{0.5}P$ using Si_2H_6," *J. Crystal Growth*, vol. 93, pp. 628–623, 1988.
[17] T. Tanaka, and S. Minagawa, "Carrier-induced refractive-index change, mode gain and spontaneous-emission factor in AlGaInP SQW-SCH laser diodes," *Electron. Lett.*, vol. 26, pp. 766–767, May 1990.
[18] H. Fujii, Y. Ueno, A. Gomyo, K. Endo, and T. Suzuki, "Observation of stripe-direction dependence of threshold current density for AlGaInP laser diodes with CuPt type natural superlattice in $Ga_{0.5}In_{0.5}P$ active layer," *Appl. Phys. Lett.*, vol. 61, pp. 737–739, Aug. 1992.
[19] Y. Ueno, "Oscillator strength enhancement for [1 1 0]-polarized light in compressively strained GaInP ordered crystals used in AlGaInP lasers," to be published in *Appl. Phys. Lett.*, vol. 62, pp. 553–555, Feb. 1993.
[20] A. Gomyo, T. Suzuki, and S. Iijima, "Observation of strong ordering in $Ga_xIn_{1-x}P$ alloy semiconductors," *Phys. Rev. Lett.*, vol. 60, pp. 2645–2648, June 1988.

Yoshiyasu Ueno received the M.S. degree in physics from the University of Tokyo, Tokyo, Japan, in 1987.

He joined NEC Corporation in 1987, and is now a researcher in the Opto-Electronics Research Laboratories, Ibaraki, Japan. He has been engaged in the research and development of AlGaInP lasers. His research interests are optical phenomena in semiconductor lasers and functional opto-electronic devices.

Mr. Ueno is a member of the Japan Society of Applied Physics and the Physical Society of Japn.

Hiroaki Fujii received the B.S. and M.S. degrees in electronics engineering from Hiroshima University, Hiroshima, Japan, in 1984 and 1986, respectively.

He joined NEC Corporation in 1986, and is now a supervisor in the Opto-Electronic Device Research Laboratory, Opto-Electronics Research Laboratories, Ibaraki, Japan. He has been engaged in the development of AlGaInP visible laser diodes, and is now mostly concentrating on the development of high-power AlGaInP laser diodes for optical recording systems.

Mr. Fujii is a member of the Japan Society of Applied Physics.

Hiroyuki Sawano received the B.S. and M.S. degrees in physics from Keio University in 1989 and 1991, respectively.

He joined NEC Corporation in 1991, and is now a researcher in the Opto-Electronic Device Research Laboratory, Opto-Electronics Research Laboratories, Ibaraki, Japan. He has been engaged in the research and development of semiconductor lasers.

Kenichi Kobayashi received the B.S. and M.S. degrees in electronics engineering from Tokyo Institute of Technology, Tokyo, Japan, in 1979 and 1981, respectively.

He joined NEC Corporation in 1981, and is now a Research Manager in the Opto-Electronic Device Research Laboratory, Opto-Electronics Research Laboratories, Ibaraki, Japan. He has been engaged in the research and development of semiconductor lasers.

Mr. Kobayashi is a member of the Japan Society of Applied Physics.

Kunihiro Hara graduated from Electrical Engineering Department, Mukaino-oka Technical High School in 1980.

He joined NEC Corporation in 1980, and is now a researcher in the Opto-Electronic Device Research Laboratory, Opto-Electronics Research Laboratories, Ibaraki, Japan. He has been engaged in developmental research on opto-electronic device processes and semiconductor lasers.

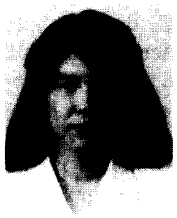

Akiko Gomyo received the B.S. degree in physics from the University of Gakushuin in 1980.

She joined NEC Corporation in 1980, and is now a supervisor of the Opto-Electronic Device Research Laboratory, Opto-Electronics Research Laboratories, Ibaraki, Japan. She has been engaged in the research and development of semiconductor opto-electronic devices and materials.

Ms. Gomyo is a member of the Japan Society of Applied Physics and of the Physical Society of Japan.

Kenji Endo received the B.S. degree in communication engineering from Tohoku University in 1976.

He joined NEC Corporation in 1976, and is now a Research Manager in the Opto-Electronic Device Research Laboratory, Opto-Electronics Research Laboratories, Ibaraki, Japan. He has been engaged in developmental research on semiconductor lasers.

Mr. Endo is a member of the Japan Society of Applied Physics and the Institute of Electronics, Information and Communication Engineers.